Laser frequency-noise-limited ultrahigh resolution remote fiber sensing

Jong H. Chow, Ian C. M. Littler †, David E. McClelland, and Malcolm B. Gray

Centre for Gravitational Physics, Faculty of Science, The Australian National University, Canberra, ACT 0200, Australia;
†Centre for Ultrahigh Bandwidth Devices for Optical Systems, School of Physics, A28, University of Sydney, Camperdown, NSW 2006, Australia

jong.chow@anu.edu.au

Abstract: When a fiber Fabry-Perot is used in an ultra-sensitive strain detection system via a radio-frequency interrogation scheme, its frequency discrimination properties can be enhanced by reducing the linewidth of its resonance. This increases the signal-to-noise ratio, and thus suppresses the strain equivalent noise floor. We demonstrate this improvement in a long-distance high performance remote sensing system and show that in reflection, it can mitigate the effects of random phase noise introduced by Rayleigh back-scattering. In transmission, it improves the remote system sensitivity to sub-picostrain resolution, which surpasses any other long-distance remote sensing system to date. With the reduced fiber Fabry-Perot linewidth, all noise sources in the delivery fiber become irrelevant, as the transmission system is limited only by the pre-stabilized laser frequency noise.

OCIS codes: (060.2370) Fiber optics sensors; (120.0280) Remote sensing; (120.3180) Interferometry

References and links

1. Jong H. Chow, Ian C. M. Littler, Glenn de Vine, David E. McClelland, and Malcolm B. Gray, "Phase-sensitive interrogation of fiber Bragg grating resonators for sensing applications," IEEE J. Lightwave Technol. **23**, 1881-1889 (2005).
2. Malcolm B. Gray, Jong H. Chow, Ian C. M. Littler, and David E. McClelland, "Ultra-High resolution strain sensing by phase-sensitive interrogation of a passive fiber Bragg resonator," Proceedings of SPIE 17th International Conference on Optical Fiber Sensors, SPIE **5855B**, 623-636, Bruges, Belgium (2005).
3. Jong H. Chow, David E. McClelland, Malcolm B. Gray, and Ian C. M. Littler, "Demonstration of a passive sub-picostrain fiber strain sensor," Opt. Lett. **30**, 1923-1925 (2005).
4. Clay K. Kirkendall, and Anthony Dandridge, "Overview of high performance fibre-optic sensing," J. Phys. D, **37**, R197-R216 (2004).
5. Alan D. Kersey, Michael A. Davis, Heather J. Patrick, Michel LeBlanc, K. P. Koo, C. G. Askins, M. A. Putnam, and E. Joseph Friebele, "Fiber Grating Sensors," J. Lightwave Technol. **15**, 1442-1463 (1997).
6. Ping Wan and Jan Conradi, "Impact of double Rayleigh backscatter noise on digital and analog fiber systems," J. Lightwave Technol. **14**, 288-297 (1996).
7. G.A. Cranch, A. Dandridge, and C.K. Kirkendall, "Suppression of double Rayleigh scattering-induced excess noise in remotely interrogated fiber-optic interferometric sensors," IEEE Photon. Technol. Lett. **15**, 1582-1584 (2003).
8. R. W. P. Drever, J. L. Hall, F. V. Kowalski, J. Hough, G. M. Ford, A. J. Munley, and H. Ward, "Laser phase and frequency stabilization using an optical resonator," Appl. Phys. B **31**, 97-105 (1983).
9. Stephane Schilt, Luc Thevenaz, and Philippe Robert, "Wavelength modulation spectroscopy: combined frequency and intensity laser modulation," Appl. Opt. **42**, 6728-6738 (2003).

#69164 - $15.00 USD Received 22 March 2006; accepted 8 May 2006

10. K Wanser, "Fundamental phase noise limit in optical fibres due to temperature fluctuations," Electron. Lett. **28**, 53-54, (1992).
11. X. Zhu, and D. Cassidy, "Modulation spectroscopy with a semiconductor diode laser by injection-current modulation," J. Opt. Soc. Am. B **14**, 1945-1950 (1997).
12. G. Gagliardi, M. Salza, P. Ferraro, P. De Natale, "Fiber Bragg-grating strain sensor interrogation using laser radio-frequency modulation," Opt. Express **13**, 2377-2384 (2005).
13. Dennis Derickson, *Fiber Optic Test and Measurement*, (Prentice Hall, Upper Saddle River, New Jersey, 1998).
14. H. Rhode, J. Eschner, F. Schmidt-Kaler, and R. Blatt, "Optical decay from a Fabry-Perot cavity faster than the decay time," J. Opt. Soc. Am. B **16**, 1425-1429 (2002).
15. Manish Gupta, Hong Jiao, and Anthony O'Keefe, "Cavity-enhanced spectroscopy in optical fibers," Opt. Lett. **27**, 1878-1880 (2002).

1. Introduction

A passive fiber Bragg grating resonator is a multi-pass optical device comprising of a pair of separated Bragg gratings, forming a fiber Fabry-Perot (FFP) interferometer. When used as a sensing element, it effectively multiplies the phase change due to minute fiber optical path displacements. It is hence an excellent frequency discriminator, with distinct advantages over a simple Bragg grating as a high performance strain sensor.

We have demonstrated its short-range interrogation in various radio-frequency (RF) laser modulation dynamic strain sensing configurations [1, 2, 3]. Remote fiber sensing, however, poses additional challenges, and various well-known difficulties must be overcome [4, 5]. RF interrogation techniques can be shown to simultaneously overcome these difficulties. They are powerful due to their immunity to laser intensity noise, as they are primarily phase-sensitive techniques. Since the laser carrier and its RF sidebands experience the same phase noise and polarization wander in the delivery fiber, these detrimental effects caused by environmental perturbations are negligible during signal extraction due to common-mode rejection. Also, passive interrogation of the FFP implies that these remote sensing systems can operate at 1550 nm in all SMF-28 fiber, thus avoiding the attenuation problems associated with long-distance pump delivery in an active fiber laser sensor. Furthermore, because the effective optical path length differences between the laser carrier and its sidebands are very small, these topologies overcome the remote interrogation length constraints imposed due to the coherence length of the laser source, as would be the case in a Mach-Zehnder or Michelson type interferometer.

One of the ultimate challenges for long-distance remote fiber sensing is the random noise effects associated with Rayleigh backscattering (RBS). These include both first-order RBS when sensing in reflection, as well as double RBS [6, 7] which persists in transmission sensing. They can degrade the sensing resolution by introducing both intensity and phase noise in high performance systems.

In this paper, we show that by improving the frequency discrimination property of the FFP resonance, the random noise effects of RBS can be mitigated by increasing the signal-to-noise ratio (SNR). We experimentally demonstrate this sensitivity improvement for reflection sensing. We also show that further strain resolution enhancement can be achieved by adopting a transmission architecture. Results for a 31 km remote fiber sensing system in transmission is presented, where sub-picostrain resolution has been attained. This ultra-high fiber strain resolution is limited only by the fundamental frequency noise of the laser. To our knowledge, this is the first frequency noise-limited long-distance remote strain sensor, where all systemic noise sources associated with the delivery fiber are effectively transparent.

2. Resonance linewidth and frequency discrimination

The error signal in a RF locking scheme is derived from the interferometric differential phase between the carrier and its modulation sidebands [8, 9]. For a fixed modulation frequency ν_m,

#69164 - $15.00 USD Received 22 March 2006; accepted 8 May 2006

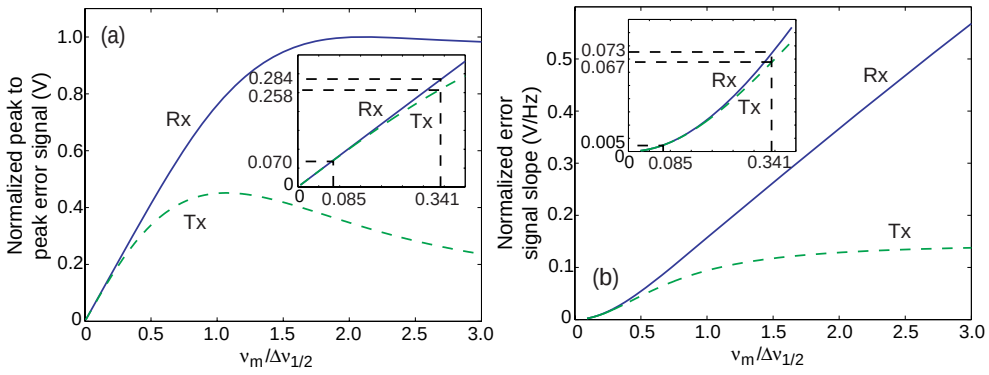

Fig. 1. (a) Theoretical normalized error signal size vs. $\nu_m/\Delta\nu_{1/2}$ ratio; and (b) error signal slope vs. $\nu_m/\Delta\nu_{1/2}$ ratio. The insets illustrate the operating regimes for the two chosen FFP resonances in our experiment.

the peak-to-peak size of this error signal, and hence the slope around its lock point, are dependent on the full-width-half-maximum (FWHM) bandwidth, $\Delta\nu_{1/2}$, of the resonance. This is illustrated in Fig. 1, where Rx denote the theoretical plots for reflection, while Tx are for transmission. Subsequent discussions regarding error signal slope throughout this paper refer to its gradient, with units of Volts/Hz, at the FFP lock point which is typically very close to resonance. When ν_m is well inside of $\Delta\nu_{1/2}$, Fig. 1a shows that the error signal size increases approximately linearly with respect to the $\nu_m/\Delta\nu_{1/2}$ ratio. On the other hand, for the same fixed ν_m, the error signal slope has a quadratic dependence on $\nu_m/\Delta\nu_{1/2}$ when $\nu_m \ll \Delta\nu_{1/2}$. This is due to the dual effect of increasing error signal size and concurrent decreasing error signal turning point frequency separation, with decrease in $\Delta\nu_{1/2}$ [1]. In this regime, a modest decrease in resonance FWHM can dramatically improve the frequency discrimination of the interrogation technique.

As $\Delta\nu_{1/2}$ reduces further, the error signal slope in reflection tends toward a linear relationship with $\nu_m/\Delta\nu_{1/2}$. This is because the error signal size, plotted in Fig. 1(a), approaches a constant value as the FWHM continues to decrease. In transmission, this slope rolls off to an asymptotic value due to the decrease in transmitted sideband power. This implies that in reflection, frequency discrimination by the FFP continues to linearly improve with increase in $\nu_m/\Delta\nu_{1/2}$, while in transmission, this improvement becomes marginal.

For a given sensing system with the same delivery fiber length and photodetector gain, the equivalent phase noise contributions associated with these parameters during signal extraction remain the same. These noises include sources such as RBS, fiber thermal noise [10], parasitic etalon effects, and electronic noise. Since the frequency discrimination by a FFP resonance can improve significantly if its FWHM is narrowed, it can enhance the SNR by yielding a larger demodulated signal for the same frequency excursion between the laser and the FFP resonance lock point. This effectively enables the signal to dominate over the strain equivalent noise contributions of all other noise sources.

3. Experimental technique

The experimental setup to demonstrate this SNR enhancement is shown in Fig. 2. We interrogated the FFP with a pre-stabilized, current modulated, external cavity diode laser. The pre-stabilized laser included its own control loop where an external cavity diode laser was locked to the resonance of a free-space confocal reference cavity by directly modulating its current at

#69164 - $15.00 USD Received 22 March 2006; accepted 8 May 2006

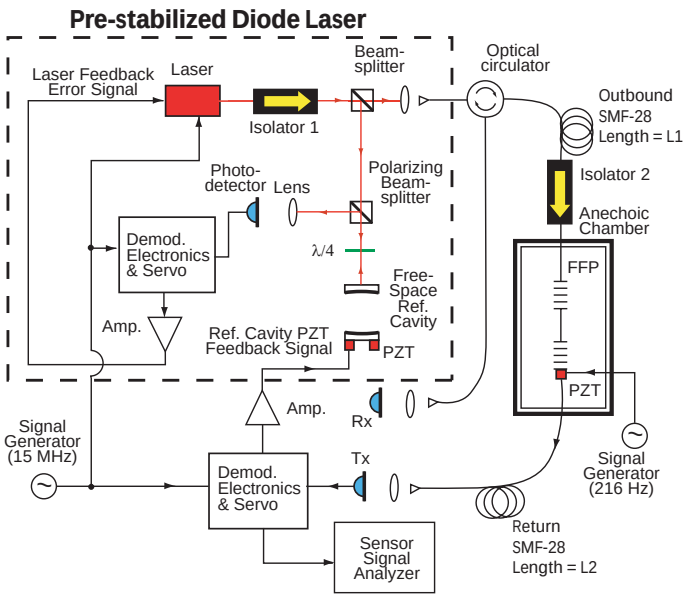

Fig. 2. Experimental setup showing the laser and stabilization cavity together with the FFP sensor in the anechoic chamber. The 15 MHz signal generator was used to modulate the current of the laser, as well as providing the local oscillator for demodulation electronics. The sensor was interrogated remotely after a fiber length of L1. For reflection sensing, the outbound and return was the same fiber, while for transmission sensing the transmitted light was detected after a further L2 of inbound fiber. Isolator 2 is present only for transmission sensing.

15 MHz. This suppresses the free-running laser noise by up to 3 orders of magnitude, in the acoustic frequency range from 10 Hz to 100 kHz. Direct current modulation [2, 11, 12] eliminates the need for an auxiliary phase modulator used in RF phase modulation techniques such as Pound-Drever-Hall frequency locking [8].

The Bragg grating pair of the FFP in this experiment each had a nominal peak reflectivity of 95%, separated by 80 mm. The gratings were not apodized, and thus exhibited a broad reflectivity roll-off near the Bragg band edges. The FFP supported several dozen modes, with differing finesse due to this varying reflectivity. By stretch tuning the FFP, therefore, the desired resonance FWHM could be chosen for comparing strain sensitivity performance, without changing other experimental parameters. One end of the FFP was attached to a PZT, allowing its length to be modulated for a direct calibration of the strain sensitivity. The FFP and its mounting were enclosed in a hermatically sealed, mechanically isolated anechoic chamber to minimize acoustic noise in the FFP.

Two configurations were investigated in this experiment. We first demonstrated performance enhancement by FFP resonance narrowing in reflection. This performance was then further improved by adopting a transmission architecture with the better frequency discriminator.

In reflection sensing, the FFP sensor was interrogated after 5 km (L1 in Fig. 2) of SMF-28 fiber, and both outbound and return light were delivered with the same fiber. In transmission, to demonstrate long-distance remote sensing, the outbound delivery fiber was extended to 21 km (L1 in Fig. 2), while the return light was transmitted with a further 10 km (L2 in Fig. 2) of SMF-28 fiber, such that the total fiber delivery length was 31 km. These fiber lengths were well beyond the coherence length of the laser, which had a factory specified intrinsic linewidth

#69164 - $15.00 USD Received 22 March 2006; accepted 8 May 2006

of $\sim$ 300 kHz, thus translating to a coherence length of $\sim$ 0.7 km. For the case of transmission sensing, a second Isolator 2 was added between the delivery fiber and the FFP. This was to eliminate parasitic etalons from forming between the macroscopic reflections off the FFP and any splice reflections upstream. The outbound and return delivery fibers were intentionally exposed to ambient laboratory and acoustic noise.

4. Results and discussion

We have chosen two FFP modes for comparison: one with $\Delta\nu_{1/2}$ of 176 MHz, near the Bragg band edge; while the other was 44 MHz, at the center of the Bragg bandwidth where the finesse was highest. The modulation frequency used was 15 MHz, and hence the $\nu_m/\Delta\nu_{1/2}$ ratios were 0.085 for $\nu_{1/2}$ of 176 MHz, and 0.341 for 44 MHz. The theoretical operating regimes for these two modes are illustrated in the insets of Fig. 1.

4.1. Reflection sensing

The corresponding reflected error signals for the low and high finesse modes are shown in Figs. 3(a) and 3(b), respectively. The theoretical and experimental ratios of FWHM, error signal peak-to-peak size, and error signal slope improvement for reflection are summarized in Table 1.

In practice, the experimental error signal size was limited by the saturation voltage of our mixer electronics. It was thus necessary to reduce the input optical power from 1 mW, when interrogating the 176 MHz mode, to 250 μW for the 44 MHz resonance, in order to maintain the error signal size at $\sim$ 1.5 V_{p-p}. Hence the experimental ratio of peak-to-peak error signal sizes between both modes was kept at $\sim$ 1. The error signal slope, and therefore the frequency discrimination in the narrower resonance was nevertheless improved by a factor of 3.3.

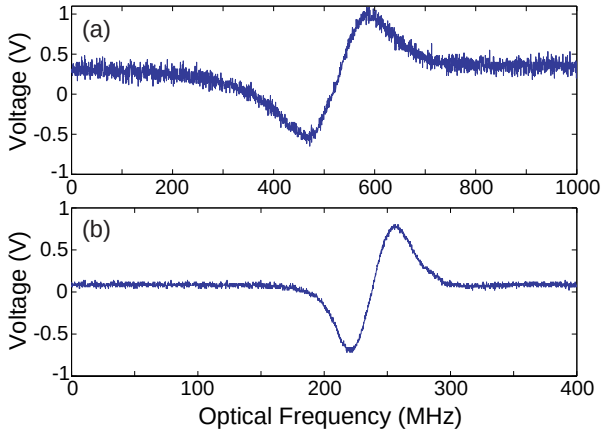

Fig. 3. Comparison between demodulated reflection error signal scans of (a) a FFP resonance with FWHM of 176 MHz, vs. (b) a FWHM of 44 MHz. In reflection, the outbound and return delivery is the same fiber of 5 km.

The absolute RBS power was substantially reduced for the high finesse mode with the lower interrogation power [13], while the absolute response to both FFP strain and frequency was increased due to the increased error signal slope. It is clear from Fig. 3 that the reflected error signal for the narrower resonance was less noisy than that obtained with a wider FWHM. This shows that narrowing of resonance linewidth can reduce the effects of first-order RBS noise in a remote fiber sensing system.

#69164 - $15.00 USD Received 22 March 2006; accepted 8 May 2006

Table 1. Summary of calculated and experimental reflected error signal ratios for our two operating regimes.

Ratio between high and low finesse modes	Calculated	Experimental
$\Delta\nu_{1/2}$	1/4	1/4
Error Signal size	4.06	~ 1
Error Signal slope	14.6	3.3

The calibrated, closed-loop strain resolution performance in reflection is shown in Fig. 4, where the strain sensitivities for the two FFP modes are overlaid. The outbound and return delivery lead was the same fiber with a length of 5 km. The strong peak at 216 Hz was our calibration signal of 0.96 n$\varepsilon/\sqrt{\text{Hz}}$. The plots demonstrate that with the narrower $\Delta\nu_{1/2}$, strain sensitivity was improved by up to an order of magnitude at lower acoustic signal frequencies. With $\Delta\nu_{1/2}$ of 44 MHz, as displayed in Fig. 4, plot (ii), the sensor exhibited a resolution of ~ 6 p$\varepsilon/\sqrt{\text{Hz}}$ at 100 Hz, improving to ~ 2 p$\varepsilon/\sqrt{\text{Hz}}$ at 100 kHz.

While the improved frequency discrimination of the FFP resonance has enhanced the sensor performance in reflection, the strain sensitivity noise floor of plot (ii) in Fig. 4 was still dominated by first-order RBS. Since there are practical limits to how far the SNR can be improved (See Section 5), one can alternatively adopt the transmission architecture to attain sub-picostrain, laser frequency noise-limited sensing.

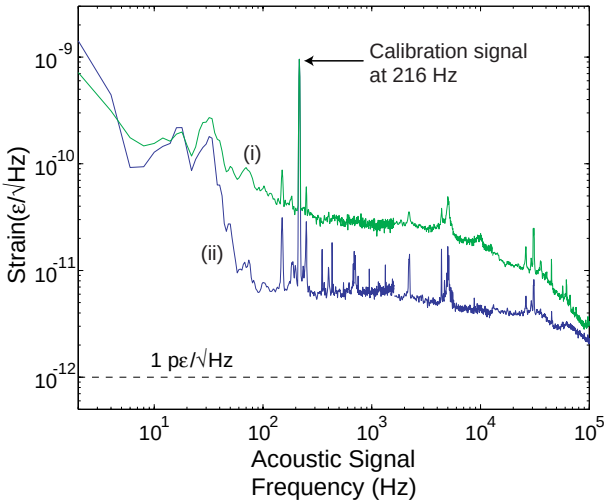

Fig. 4. The calibrated noise spectra of the fiber Fabry-Perot sensor in reflection, with the same outbound and return fiber of 5 km, using a resonance $\Delta\nu_{1/2}$ of (i) 176 MHz; and (ii) 44 MHz, when interrogated remotely by RF current modulation of the diode laser. An external mechanical signal of 0.34 nm at 216 Hz was applied to the FFP via a PZT.

4.2. Transmission sensing

In transmission, the system would not be affected by first-order RBS. With the isolator placed between the outbound delivery fiber and the FFP, all macroscopic etalons are additionally eliminated, leaving only double RBS effects. The narrower FFP resonance facilitates sufficient SNR

#69164 - $15.00 USD Received 22 March 2006; accepted 8 May 2006

to then bury this secondary effect below the residual laser frequency noise.

Table 2. Summary of calculated and experimental transmitted error signal ratios for our two operating regimes.

Ratio between high and low finesse modes	Calculated	Experimental
$\Delta\nu_{1/2}$	1/4	1/4
Error Signal size	3.69	~ 1
Error Signal slope	13.4	3.1

The theoretical and experimental ratios of FWHM, error signal peak-to-peak size, and error signal slope improvement for transmission are summarized in Table 2. As in the case of reflection, the ratio of transmitted peak-to-peak error signal sizes between the two modes was kept at ~ 1. The error signal slope nevertheless showed an improvement by a factor of 3.1, while the reduction in laser interrogation power reduces double RBS absolute noise power accordingly.

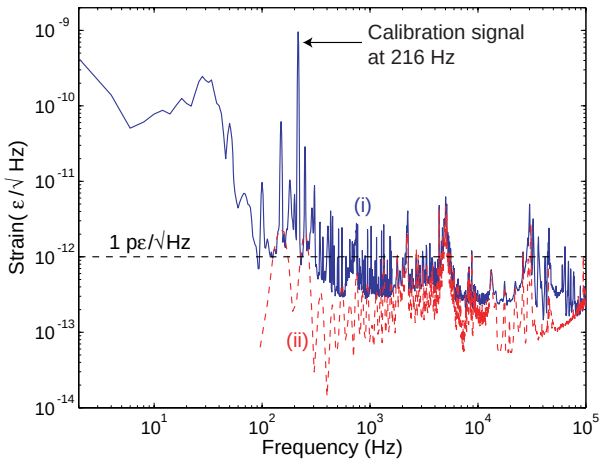

Fig. 5. (i) The calibrated noise spectrum of the Fiber Fabry-Perot sensor in transmission when its resonance $\Delta\nu_{1/2}$ of 44 MHz was interrogated remotely by RF current modulation of the diode laser after 21 km of fiber. It is overlaid with (ii) the strain equivalent frequency noise of the pre-stabilized laser. The transmitted light was returned via a further 10 km of inbound delivery fiber before detection and demodulation.

The closed-loop strain resolution spectrum in transmission for the high finesse mode is displayed in Fig. 5. The outbound fiber was 21 km long, while the return fiber was 10 km. Despite 31 km of total round-trip SMF-28 fiber, this system demonstrated sub-picostrain sensitivity to acoustic signal frequencies from about 300 Hz to 100 kHz. This superior sensitivity plot is overlaid with the strain equivalent pre-stabilized laser frequency noise. It can be seen that this narrow FWHM remote sensing system is very nearly limited by the closed-loop frequency noise of the pre-stabilized laser, and the various noise sources associated with the 31 km of delivery fiber are now transparent to the interrogation architecture. Further optimization of system performance would require frequency noise improvement of the laser source. This can be done either by improving the pre-stabilization of the diode laser, or by switching to an inherently narrower linewidth source such as a fiber laser.

#69164 - $15.00 USD
Received 22 March 2006; accepted 8 May 2006

5. Practical limits to resonance linewidth narrowing

There are practical limits to how narrow $\Delta\nu_{1/2}$ can be reduced and still improve system performance. In Fig. 1(b), we see that in transmission, the error signal slope does not increase significantly after $\nu_m/\Delta\nu_{1/2}$ exceeds unity. In reflection, this frequency discrimination in theory continues to improve as the FWHM narrows. As $\Delta\nu_{1/2}$ approaches the linewidth of the laser, however, the fundamental fluctuations of the laser frequency would be beyond the linear range of the error signal [14]. If the FWHM reduces further, these fluctuations would be beyond the dynamic range of the sensor. Another practical limitation is the typical emergence of non-degeneracy in polarization modes as the linewidth of a FFP resonance reduces [15]. In a sensing architecture that is not polarization-maintaining, polarization fading can then result in significant change in the error signal slope. The system is then no longer immune to ambient perturbations in the delivery fiber, and these perturbations would couple into the signal readout as random changes in strain sensitivity.

6. Conclusion

Using a narrow FWHM FFP strain sensor, we have achieved a sensitivity of 6 p$\varepsilon/\sqrt{\text{Hz}}$ in reflection at an interrogation distance of 5 km, for a total round-trip delivery fiber length of 10 km. In transmission, we attained sub-picostrain resolution with 31 km of total remote delivery fiber. With the narrow FWHM FFP, all noises sources in the 31 km delivery fiber become irrelevant, as the transmission system is limited only by the pre-stabilized laser frequency noise. This is a major step towards the realization of ultra-sensitive, long-distance remote fiber sensing. We note that the sensitivity is not limited by the 31 km of fiber, although fundamental attenuation in SMF-28 fiber would place a practical limit on this system to an outbound and return total remote sensing length of about 100 km.

Acknowledgments

This research was primarily supported by the Australian Research Council (ARC) under the auspices of the Australian Consortium for Interferometric Gravitational Astronomy, with partial assistance from the ARC Centres of Excellence Program through the Centre for Ultrahigh Bandwidth Devices for Optical Systems (CUDOS). The authors would like to thank Dr. Ping Koy Lam for the loan of the 21 km of SMF-28 fiber.

#69164 - $15.00 USD Received 22 March 2006; accepted 8 May 2006